Cerebral Cortex, May 2019;29: 1984–1996

doi: 10.1093/cercor/bhy077
Advance Access Publication Date: 13 April 2018
Original Article

ORIGINAL ARTICLE

Association Between Brain Activation and Functional Connectivity

Dardo Tomasi[1] and Nora D. Volkow[1,2]

[1]National Institute on Alcohol Abuse and Alcoholism, Bethesda, MD 20892, USA and [2]National Institute on Drug Abuse, Bethesda, MD 20892, USA

Address correspondence to Dardo Tomasi, Laboratory of Neuroimaging (LNI/NIAAA), 10 Center Dr, Rm B2L124, Bethesda, MD 20892-1013, USA.
Email: dardo.tomasi@nih.gov

Abstract

The origin of the "resting-state" brain activity recorded with functional magnetic resonance imaging (fMRI) is still uncertain. Here we provide evidence for the neurovascular origins of the amplitude of the low-frequency fluctuations (ALFF) and the local functional connectivity density (lFCD) by comparing them with task-induced blood-oxygen level dependent (BOLD) responses, which are considered a proxy for neuronal activation. Using fMRI data for 2 different tasks (Relational and Social) collected by the Human Connectome Project in 426 healthy adults, we show that ALFF and lFCD have linear associations with the BOLD response. This association was significantly attenuated by a novel task signal regression (TSR) procedure, indicating that task performance enhances lFCD and ALFF in activated regions. We also show that lFCD predicts BOLD activation patterns, as was recently shown for other functional connectivity metrics, which corroborates that resting functional connectivity architecture impacts brain activation responses. Thus, our findings indicate a common source for BOLD responses, ALFF and lFCD, which is consistent with the neurovascular origin of local hemodynamic synchrony presumably reflecting coordinated fluctuations in neuronal activity. This study also supports the development of task-evoked functional connectivity density mapping.

Key words: ALFF, BOLD, HCP, lFCD, neurovascular

Introduction

Resting functional connectivity (FC) (Biswal et al. 1995), a powerful tool to assess neuropsychiatric disorders in absence of task conditions (Fox et al. 2006; Greicius 2008), is based on spontaneous fluctuations in blood-oxygen level dependent (BOLD) signals measured with functional magnetic resonance imaging (fMRI). Whereas the task-based BOLD signal is considered a proxy for neuronal activity (Logothetis et al. 2001), the origin of the spontaneous brain activity is less certain, and the interpretation of changes in resting-state activity, reflecting complex combination of neural, vascular, and metabolic factors, is not always straightforward (Liu 2013). Specifically, previous studies showing reduced resting-state signals after pharmacological manipulations with stimulant drugs (caffeine and cocaine) and hypercapnia suggest that the resting-state fMRI signal is dominated by cerebral blood flow (Biswal et al. 1997; Li et al. 2000; Rack-Gomer et al. 2009; Murnane et al. 2015; Wong et al. 2012; Vélez-Hernández et al. 2014). However, the spontaneous BOLD signals show correlation with locally measured neuronal activity (Shmuel and Leopold 2008) in the upper gamma frequency band (Magri et al. 2012), similar to the observed correlation between local neuronal activity and spontaneous fluctuations in cortical cerebral blood volume (Schölvinck et al. 2010).

A popular technique used for the analysis of the spontaneous fluctuations is based on regions-of-interest (ROIs) (seed regions) and correlation analyses (Biswal et al. 1995). The strength of the correlations between functionally connected regions have shown linear associations with cerebral blood flow data obtained using arterial spin labeling (Liang et al.

2013), and with the alpha power of electroencephalography data (Chang et al. 2013) simultaneously collected with BOLD–fMRI data, providing additional evidence for the neurovascular origin of spontaneous BOLD fluctuations. The evidence supporting the neurovascular origin of the amplitude of low-frequency fluctuations (ALFF) and other voxelwise FC metrics is more limited. Though the associations of ALFF and local functional connectivity density (lFCD) with brain glucose metabolism, a marker of neuronal activity (Sokoloff et al. 1977), suggest that resting-state FC metrics also have neuronal origin (Tomasi et al. 2013).

lFCD quantifies local degree, the size of the local network cluster functionally connected to a brain network node and is a powerful voxelwise data-driven tool for exploring the topology of the human brain connectome. In contrast to seed-voxel correlation analysis, ultrafast lFCD is ideal for exploratory analyses in large datasets (Biswal et al. 2010; Tomasi and Volkow 2010, 2012a). lFCD is proportional to local energy utilization (Tomasi et al. 2013) and sensitive to aging (Tomasi and Volkow 2012b), gender (Tomasi and Volkow 2011), stimulant drugs (Konova et al. 2015), intelligence (Lang et al. 2015), brain development (Tomasi and Volkow 2014), and dopamine signaling (Tian et al. 2013). lFCD was shown to be disrupted in attention deficit hyperactivity disorder (Tomasi and Volkow 2012a), cocaine addiction (Konova et al. 2015), nonepileptic seizures (Ding et al. 2014), schizophrenia (Tomasi and Volkow 2014; Liu et al. 2015; Zhuo et al. 2014), congenital blindness (Qin et al. 2015), and traumatic axonal injury (Caeyenberghs et al. 2015). However, lFCD results may not purely reflect local correlations of activity in a neuronal population, but may instead be affected by vascular confounds such as correlations in local vascular structure (Logothetis et al. 2009). The goal of the present study was to assess the coupling between neurovascular responses and lFCD during task conditions as well as after the removal of task-related signal modulations.

We assessed the correlations of the task-related BOLD signal change, a proxy for neural activity (Logothetis et al. 2001), with lFCD and the amplitude of low-frequency fluctuations (ALFF) (Yang et al. 2007) during task-based fMRI. Our hypothesis was that brain regions activated by the tasks would show increased lFCD in proportion to the task-related BOLD signal changes. We further hypothesized that this association would be reproducible and stronger for lFCD than for ALFF, given the vascular nature of ALFF (Di et al. 2013). Here we test these hypotheses using task-based fMRI data from 426 subjects of the Human Connectome Project (HCP) and demonstrate the neurovascular origin of the lFCD, indirectly, through its association with the task-related BOLD signal.

Methods

Subjects

Data were drawn from the publicly available repository of the WU-Minn HCP 500 Subjects data release (http://www.humanconnectome.org/). The scanning protocol was approved by Washington University in St. Louis's Human Research Protection Office (HRPO), IRB# 201 204 036. No experimental activity with any involvement of human subjects took place at the author's institutions. The 523 subjects included in the HCP 500 Subjects data release provided written informed consent as approved by the IRB at Washington University. In total, 97 of the subjects were excluded from the study due to incomplete image datasets, image artifacts (identified with the aid of principal component analysis), or excessive head motion (mean framewise displacement > 0.4 mm). The remaining 426 participants (age: 29 ± 4 years; 244 females) were included in this study and classified into group 1 (grp1; subject# < 203500), for initial testing, or group 2 (grp2; subject# > 203500) for corroboration.

fMRI Tasks

We selected fMRI datasets collected during the performance of 2 different tasks, Social cognition and Relational processing, which are described in details elsewhere (Barch et al. 2013). We selected these 2 out of the 7 tasks used by the HCP because despite their targeting very different cognitive domains, these visual tasks cause similar brain activation patterns (Barch et al. 2013), making it possible to study the association between brain activation and the strength of the FC metrics across cognitive domains.

Social Cognition Task

The 23 s-long video clips of objects (squares, circles, triangles) either interacting in some way ("Social" video clip) or moving randomly ("Random" video clip) (Castelli et al. 2000; Wheatley et al. 2007) were shown to the subjects. Then, the subjects decided whether the movement of the objects reflected: 1) a social; 2) uncertain, or 3) no interaction among them. Each of the 2 task runs had 5 video blocks (2 "social" and 3 "random" epochs in one run, 3 "social" and 2 "random" epochs in the other run) and 5 fixation blocks (15s each). The total scan time for the Social task was 2 × 197s = 394s.

Relational Processing

This task was shown to engage the rostrolateral prefrontal cortex, defined as the lateral portion of Brodmann area (BA) 10 (Smith et al. 2007), which appears to be involved in complex cognitive functions (i.e., reasoning, working, and episodic memory). The participants were presented with 2 pairs of objects, each of them having 1 of 6 different shapes filled with 1 of 6 different textures. One pair was presented at the top and the other pair at the bottom of the screen. During "relation" epochs the participant was instructed to first decide what dimension (shape or texture) differs across the top pair of objects and then whether the bottom pair of objects also differs along that same dimension. During control "match" epochs, they saw 2 objects at the top of the screen and one object at the bottom of the screen, and a word in the middle of the screen (either "shape" or "texture"). The subject was instructed to decide whether the bottom object matched either of the top 2 objects on that dimension. The stimuli were presented for 2800 ms with 400 ms inter trial intervals and 5 trials per block. In each of the 2 runs of this task, there were 3 "relation", 3 "match" and 3 "fixation" blocks, each one lasting 16s. The total scan time of the Relational task was 2 ×167s = 334s.

MRI Acquisition and Precomputed HCP Image Analyses

Resting-state functional images were acquired in a 3.0 T Siemens Skyra unit with a 32-channel coil while the participant relaxed with eyes open using a gradient-echo-planar (EPI) sequence with multiband factor 8, TR 720 ms, TE 33.1 ms, flip angle 52°, 104 × 90 matrix size, 72 slices, and 2 mm isotropic voxels (Smith et al. 2013; Uğurbil et al. 2013). Scans were repeated twice using left–right (LR) and right–left (RL) phase encoding directions.

The "minimal preprocessing" datasets, which include gradient distortion correction, rigid-body realignment, field-map processing and spatial normalization to the stereotactic space of the Montreal Neurological Institute (MNI) (Glasser et al. 2013) were used in this work. In addition, the HCP's gray and white matter parcellations ("wmparc") of each subject's brain structural scans were used to define the anatomical seed region (pericalcarine cortex) for seed-voxel correlation analyses (see below).

Pipelines

The following preprocessing steps were carried out using IDL (ITT Visual Information Solutions, Boulder, CO). Four pipelines were used for ALFF and 8 for lFCD (Fig. 1A). Six out of the 12 pipelines included global signal regression. All pipelines included a step to minimize motion related fluctuations in MRI signals, which was based on multilinear regression and the time-varying realignment parameters (Tomasi and Volkow 2010). The lFCD included low-pass filtering (0.10 Hz frequency cutoff) to attenuate physiologic noise of high-frequency components (Cordes et al. 2001), which was not necessary for ALFF.

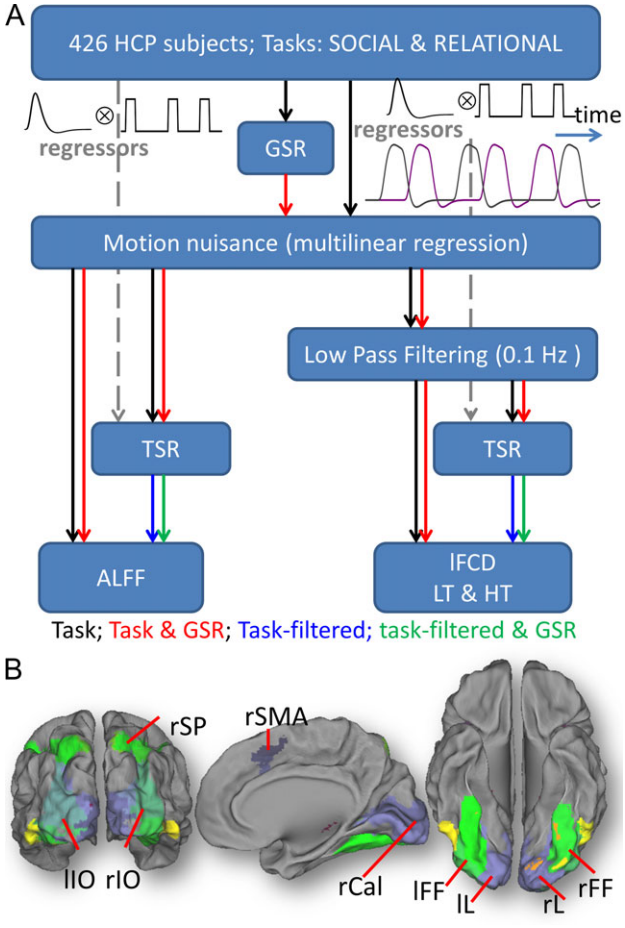

Figure 1. Pipelines and ROIs. (*A*) Local functional connectivity density (lFCD), and amplitude of low-frequency fluctuations (ALFF) maps with 2-mm isotropic resolution were computed for 426 subjects from the HCP 500 data release (see text). GSR: global signal regression; TSR: task signal regression. LT and HT: low (<0.4) and high (<0.6) correlation thresholds. (*B*) Nine regions-of-interest (ROIs) were defined as intersections between the anatomical partitions in the AAL atlas and the group-level fMRI activation patterns for the Relational task, thresholded at *t*-score = 20. lL and *r*L: left and right lingual gyri; lIO and *r*IO: left and right inferior occipital gyri; lFF and *r*FF: left and right fusiform gyri; *r*SP: right superior parietal cortex; *r*SMA: right supplementary motor area; and rCal: right pericalcarine cortex.

Task signal regression (TSR) was used in 6 of the pipelines to assess the effect of task-related BOLD signal changes. Note that the HCP 500 Subjects data release includes the onset and duration of the tasks epochs for each of the fMRI task and runs (LR and RL), which were used to regress out task-related BOLD signal changes as previously proposed (Whitfield-Gabrieli and Nieto-Castanon 2012; Di et al. 2015). Specifically, we assumed a "boxcar" design (i.e., a constant level of neural activity during the epochs) defined by the onsets and durations of the task epochs, independently for each condition ("social"/"random"; "relation"/"match"). To obtain task regressors, the boxcar time courses were convolved with a canonical hemodynamic response function (HRF) based on the sum of 2 gamma probability density functions, computed using the Matlab (MathWorks, Inc., Natick, MA) script spm_volterra.m from SPM12 (Wellcome Trust Center for Neuroimaging, London, UK). Like in standard approaches used to remove motion and global nuisances, multilinear regression was used to regress out the signal modulation induced by the fMRI tasks. Specifically, linear regression was used to fit a multilinear model for the zero-mean signal time course at a voxel location $\mathbf{r}$, $S(\mathbf{r},t)$, with the task regressors $R_i(\mathbf{r},t)$ as the independent variables:

$$S(\mathbf{r}, t) = \sum_{i=1}^{2} \beta_i R_i(\mathbf{r}, t) + \xi(\mathbf{r}, t), \quad (1)$$

where β_i are the adjustable model parameters (slopes) and $\xi(\mathbf{r},t)$ is the residual or "task-filtered" time course. In addition, we implemented a control condition for the "task-filtered" metrics in which the TSR regressors were delayed 0–20s (Δ) using a uniform random number generator,

$$S(\mathbf{r}, t) = \sum_{i=1}^{2} \beta_i' R_i(\mathbf{r}, t + \Delta) + \xi'(\mathbf{r}, t), \quad (2)$$

where $\beta_i \neq \beta_i'$ and $\xi(\mathbf{r},t) \neq \xi'(\mathbf{r},t)$.

lFCD

The lFCD was computed as the number of elements in the local FC cluster using a "growing" algorithm written in IDL (Tomasi and Volkow 2010). The Pearson correlation was used to assess the strength of the FC, R_{ij}, between voxels i and j in the brain, and a correlation threshold was selected to ensure significant correlations between time-varying signal fluctuations are corrected at $P_{FWE} < 1E\text{-}06$. A voxel (x_j) was added to the list of voxels functionally connected with x_0 only if it was adjacent to a voxel that was linked to x_0 by a continuous path of functionally connected voxels and $R_{0j} > 0.4$ (LT) or > 0.6 (HT). This calculation was repeated for all brain voxels that were adjacent to those that belonged to the list of voxels functionally connected to x_0 in an iterative manner until no new voxels could be added to the list. Note that lFCD was evaluated in the whole brain without any masking procedure (number of voxels > 2E+05). Lastly, the logarithm of lFCD was computed to normalize its distribution across subjects. Thus, 8 pipelines mapped lFCD (with/without GSR; with/without TSR; LT/HT).

ALFF

The fast Fourier transform was used to compute ALFF as the average of the power spectrum's square root in the 0.01–0.10 Hz

frequency bandwidth (Yang et al. 2007). Four pipelines were used to map ALFF (with/without GSR; with/without TSR).

fMRI Activation

The HCP 500 Subjects data release includes precomputed subject-level analyses (fixed effects) in volume space combining the 2 runs (LR and RL) for each task. These contrasts were used to assess brain activation at the group-level in this work. Specifically, the estimated fMRI contrasts with 4 mm spatial smoothing were considered individually as well as averaged to map the overall BOLD signal changes, independently for each task and subject. One-sample *t*-test and paired *t*-test, carried with the statistical parametric mapping package SPM12, were used to assess the statistical significance of task-related BOLD signal changes across subjects, independently for each task. Stringent statistical criteria for multiple comparison corrections based on the random field theory and familywise (FWE) rate at the $P_{FWE} < 0.05$ at the voxel-level and a minimum cluster size of 100 voxels were used (Eklund et al. 2016).

Region-of-Interest Analyses

To assess the association between connectivity changes and BOLD changes induced by the tasks we used the following anatomical-functional ROI approach based on the Automated Anatomical Labeling (AAL) atlas (Tzourio-Mazoyer et al. 2002) and the fMRI activation patterns. Using IDL, the ROIs were defined as the intersections between the anatomical partitions in the AAL atlas and the group-level statistical *t*-score maps of fMRI activation, thresholded at *t*-score = 20 (Cohen's $d \sim 2$) that had volumes larger than 20 voxels (160 uL). Due to the nature of the brain activation patterns most ROIs were located in occipital visual areas. For the sake of clarity and simplicity here we focus on 9 ROIs that were strongly activated by both the Social and the Relational tasks: left and right lingual (*l*L and *r*L), inferior occipital (*l*IO and *r*IO), and fusiform (*l*FF and *r*FF) gyri, right supplementary motor area (*r*SMA), superior parietal (*r*SP) and pericalcarine (*r*Cal) cortices. Figure 1*B* and Supplementary Figure S1 highlight the ROIs. In addition, we used the functional partitions of cerebral cortex in the Gordon Atlas which fit known network structures (Gordon et al. 2016) to assess the statistical distribution of task-related BOLD and *l*FCD changes in 10 major networks: the cingulum–operculum (CON), auditory (AUN), default-mode (DMN), dorsal (DAN) and ventral (VAN) attention, visual (VIN), hand (SMH) and mouth (SMM) sensorimotor, frontoparietal (FPN), and retrosplenial–temporal (RTN) networks. The connectivity metrics and the BOLD signal changes induced by the tasks were averaged within these ROIs.

Statistical Analyses

The connectivity metrics were spatially smoothed using a 4 mm gaussian kernel using fslmath to match the spatial smoothing of the fMRI activation maps. Then we used paired *t*-test to assess the statistical significance of task-related changes in connectivity between sessions and linear regression to assess their association with the BOLD signals elicited by the tasks. SPM12 was used for these purposes. Statistical significance was set by a $P_{FWE} < 0.05$, cluster-level corrected for multiple comparisons using the random field theory and a familywise error correction with a cluster-defining threshold $P < 0.001$ and a minimum cluster size of 200 voxels, following current standards (Eklund et al. 2016).

Results

Behavior

The average framewise displacement (Power et al. 2012), FD, during the fMRI task did not differ significantly between the Social (FD = 0.16 ± 0.07 mm) and Relational (FD = 0.17 ± 0.08 mm) tasks or between group 1 and group 2 ($P > 0.11$; Fig. S2A). Accuracy was lower and reaction time higher for the Relational than for the Social task ($P < 1E\text{-}58$).

fMRI Activation

The Relational task predominantly activated visual, parietal, and prefrontal regions (Fig. 2*A*). In all ROIs, the %BOLD signal changes induced by the task fitted a normal distribution across subjects (average skewness = 1.6 and kurtosis = 2.6 across ROIs; Fig. 2*B*). The %BOLD signals were strongest in the pericalcarine cortex (Fig. 2*C*). Similar results emerged for the Social task (Figs S3 and S4) and were highly reproducible across groups (Fig. 2*D* and Fig. S5). For the Relational task, the mean and the standard deviation of the %BOLD signals were correlated across ROIs, such that ROIs with higher mean also have higher standard deviation ($R = 0.82$; $P = 0.007$, 2-tailed); for the Social task, however, the correlation between the mean and the standard deviation was not significant ($R = 0.54$, $P = 0.13$). The tasks also deactivated the default-mode network. However, since the origin of the negative BOLD responses is still controversial (Tomasi et al. 2006; Singh and Fawcett 2008; Klingner et al. 2010; Walter et al. 2016), the study of the association between connectivity and BOLD signals within deactivated regions is far more complex and not within the scope of this study.

lFCD

The *l*FCD patterns fitted tightly the cortical gray matter patterns in all subjects, both without and with TSR. As expected, the TSR approach attenuated task-related modulations in the BOLD signal time courses in all subjects (Fig. 3*A*,*B*; see also Fig. S6 for similar attenuations for the Relational task), which decreased the strength of the *l*FCD. The average *l*FCD across subjects was highly symmetrical in the left and right brain hemispheres, with or without TSR (i.e., with or without task-related BOLD signal modulation, respectively; Figs 4*A* and S7*A*). It was higher in occipital, superior, inferior, and posterior (precuneus and angular gyrus) parietal cortices (*l*FCD > 3; Fig. 4*A*) than in other brain regions. The average *l*FCD across ROIs had an approximately normal distribution, both (average skewness = 0.7 and kurtosis = 0.4 across ROIs) with and without ("task-filtered"; skewness = 4.0; kurtosis = 0.9) task-related BOLD signals (Figs 4*B* and S7*B*). The average *l*FCD showed higher strength for task than for task-filtered conditions. Similar results were obtained for each of the ROIs (Fig. 4*C*) as well as for the Social task (Fig. S7*C*), showing consistent effects of task performance on *l*FCD across ROIs, and for groups 1 and 2 (Figs 4*D* and S7*D*), demonstrating reproducibility for the effect of TSR across groups of subjects and across fMRI tasks. *l*FCD values computed with or without TSR were highly correlated across ROIs, such that ROIs with higher mean *l*FCD without TSR also had higher mean *l*FCD with TSR (Relational: $R = 0.91$; $P = 7E\text{-}04$; Social: $R = 0.96$; $P = 4E\text{-}05$).

During the Relational task, the task-related increases, Δ*l*FCD, mapped as the difference in *l*FCD between "task" and "task-filtered" conditions, had normal distribution (average skewness = 0.9 and kurtosis = 0.8), were statistically significant

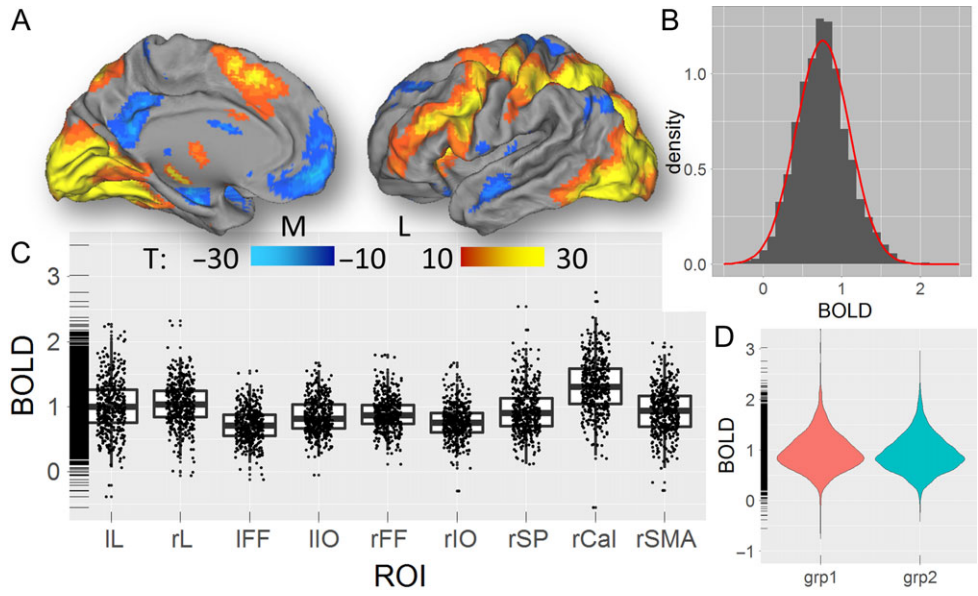

Figure 2. fMRI activation. (*A*) Statistical significance of the average BOLD signal changes induced by the "relation" and "match" epochs of the Relational task across 426 subjects of the HCP, superimposed on medial (M) and lateral (L) views of the left cortical hemisphere of the population-average Landmark- and Surface-based (PALS-B12) atlas of the cerebral cortex (Van Essen 2005). (*B*) Probability distribution of task-related %BOLD signal changes across subjects, averaged across ROIs (gray histogram) and the corresponding normal distribution (red curve). (*C*) Boxplot showing the average %BOLD signal change for each subject within each ROI. (*D*) Violin plot showing the reproducibility of the average %BOLD signal changes in groups 1 ($N = 213$) and 2 ($N = 213$). The rug plot visualization (*C* and *D*) supplement the 2d displays with 1d marginal distributions. *l*L and *r*L: left and right lingual gyri; *l*IO and *r*IO: left and right inferior occipital gyri; *l*FF and *r*FF: left and right fusiform gyri; *r*SP: right superior parietal cortex; *r*SMA: right supplementary motor area; and *r*Cal: right pericalcarine cortex.

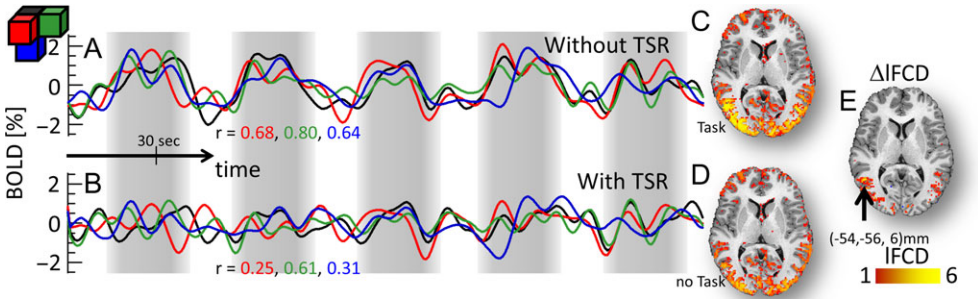

Figure 3. Individual effect of task signal regression (TSR) on lFCD. Left: Exemplary single-subject %BOLD signal time courses without (*A*) and with (*B*) TSR for 4 adjacent voxels (black, red, green, and blue waves and cubes) in the middle temporal gyrus (black arrow in *E*) for the Social task. Right: Corresponding lFCD without (*C*) and with (*D*) the task-related lFCD-increases (*E*) superimposed on an axial view of the T1-weighted MRI structure of the subject's brain. The vertical gray patterns highlight the regressors corresponding to the onsets and durations of "social" and "random" epochs. The correlations between the signal time course at (−54, −54, 6) mm (black wave) and those in adjacent voxels (r; red, green and blue labels) decrease with TSR, compared to without TSR, reflecting the attenuation of task-related modulations in the amplitude of the BOLD signal (A) with TSR (B).

($P_{FWE} < 0.05$) in most brain areas that showed significant fMRI activation (Fig. 4*E*), were reproducible across groups and paralleled the distribution of BOLD responses across functional networks (Fig. 4*F*). Similar results emerged for the Social task (Figs S8 and S9). Likewise, for the task-related BOLD signal and for the Δ*l*FCD the mean and the standard deviation were highly correlated across ROIs, such that ROIs with higher mean also had a higher standard deviation (Relational: $R = 0.98$; $P < 5E\text{-}06$; Social: $R = 0.82$; $P < 0.007$).

Association Between lFCD and BOLD

Without TSR, lFCD showed strong correlations with BOLD signals elicited by the Relational task in most brain regions that demonstrated significant activation (Fig. 5*A*–*C*). With TSR, however, lFCD showed weaker correlations with BOLD signals elicited by the Relational task in all ROIs ($P < 1E\text{-}04$), and in most brain regions that demonstrated significant activation. Differently, random TSR did not decrease significantly the association between lFCD and BOLD signals for the Relational task. Similar results emerged for the Social task (Fig. S10).

Correlation Threshold and GSR

Whereas the association between task-related BOLD signal changes and lFCD computed with GSR was significant in all ROIs (Fig. 5*D*–*F*; $P < 3E\text{-}05$), GSR significantly reduced the association with BOLD, compared to no-GSR, in all ROIs ($P < 0.008$, 2-tailed). Differently, the association between task-related BOLD signal changes and lFCD did not differ significantly as a function of correlation thresholds in any ROI (Fig. 5*E*,*F*).

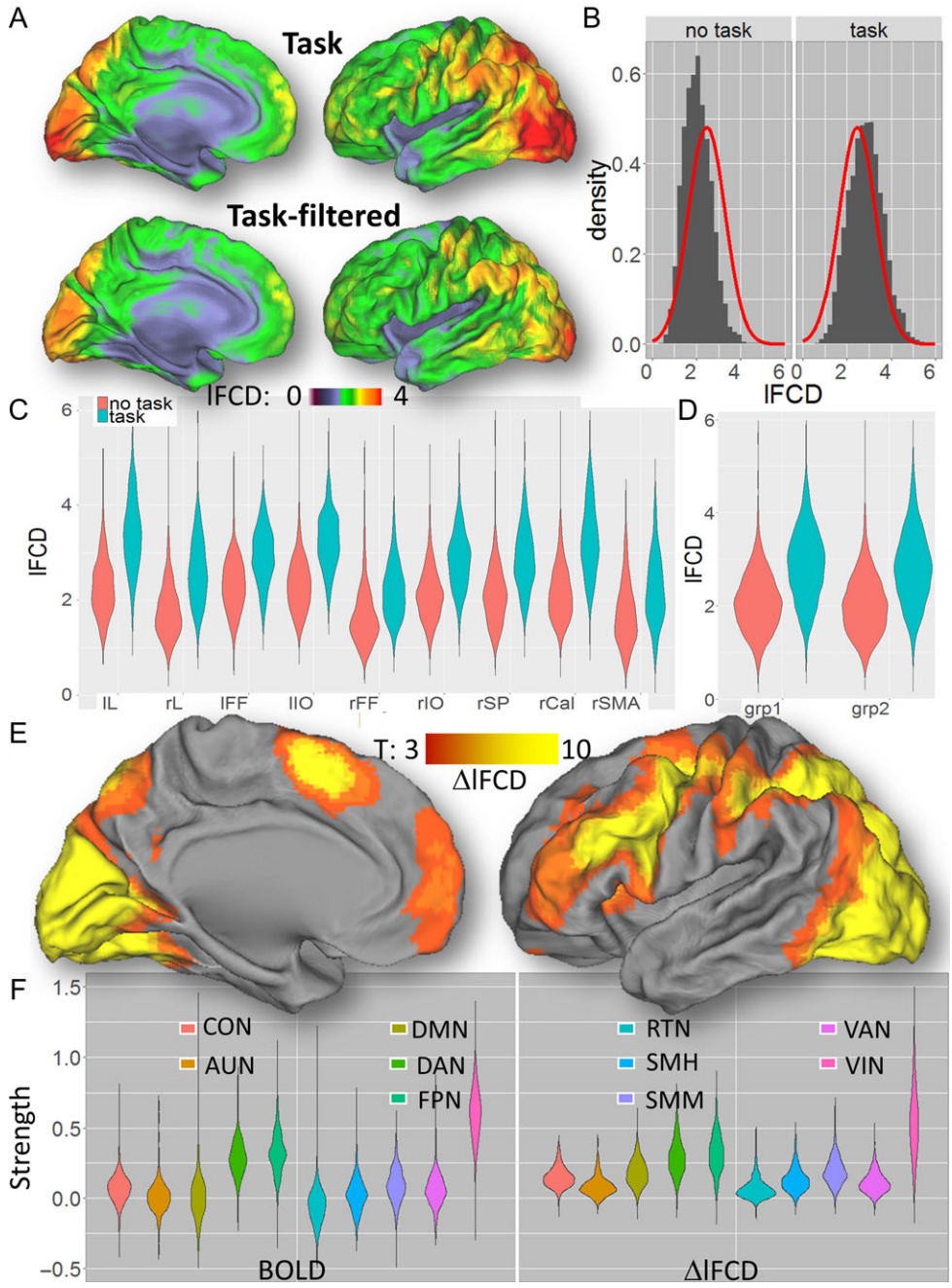

Figure 4. Effects of the relational task on lFCD. (*A*) Average lFCD distributions across 426 subjects for the Relational task, with (task) and without (task-filtered) TSR, superimposed on medial and lateral views of the left cortical hemisphere of the PALS-B12 atlas of the cerebral cortex. (*B*) Probability distributions of lFCD across subjects without (task) and with (task-filtered) TSR, averaged across ROIs (gray histograms) and the normal distributions (red curves) corresponding to their average. Violin plots showing the average lFCD for each ROI (*C*) and group (*D*) with and without TSR. (*E*) Statistical significance of task-related changes in lFCD (i.e., from "task" to "task-filtered" conditions), ΔlFCD, across 426 subjects for the Relational task. (*F*) Violin plot showing the average BOLD and ΔlFCD for each functional network. Anatomical parcels: lL and rL: left and right lingual gyri; lIO and rIO: left and right inferior occipital gyri; lFF and rFF: left and right fusiform gyri; rSP: right superior parietal cortex; rSMA: right supplementary motor area; and rCal: right pericalcarine cortex. Functional networks: cingulum-operculum (CON), auditory (AUN), default-mode (DMN), dorsal (DAN) and ventral (VAN) attention, visual (VIN), hand (SMH) and mouth (SMM) sensorimotor, frontoparietal (FPN), and retrosplenial-temporal (RTN).

ALFF Versus BOLD

During the Relational task, the task-related increases in ALFF (ΔALFF) were reproducible, strong and statistically significant in the whole brain, without and with GSR (Fig. S11). The linear associations with BOLD were weak for ALFF (Fig. 6) and strong for ΔALFF in all ROIs (Fig. S11), and random TSR did not change significantly the association between ALFF and BOLD signals (not shown). Like for lFCD, ΔALFF had normal distributions across subjects in all ROIs (Fig. S12). Similar results emerged for the Social task (not shown).

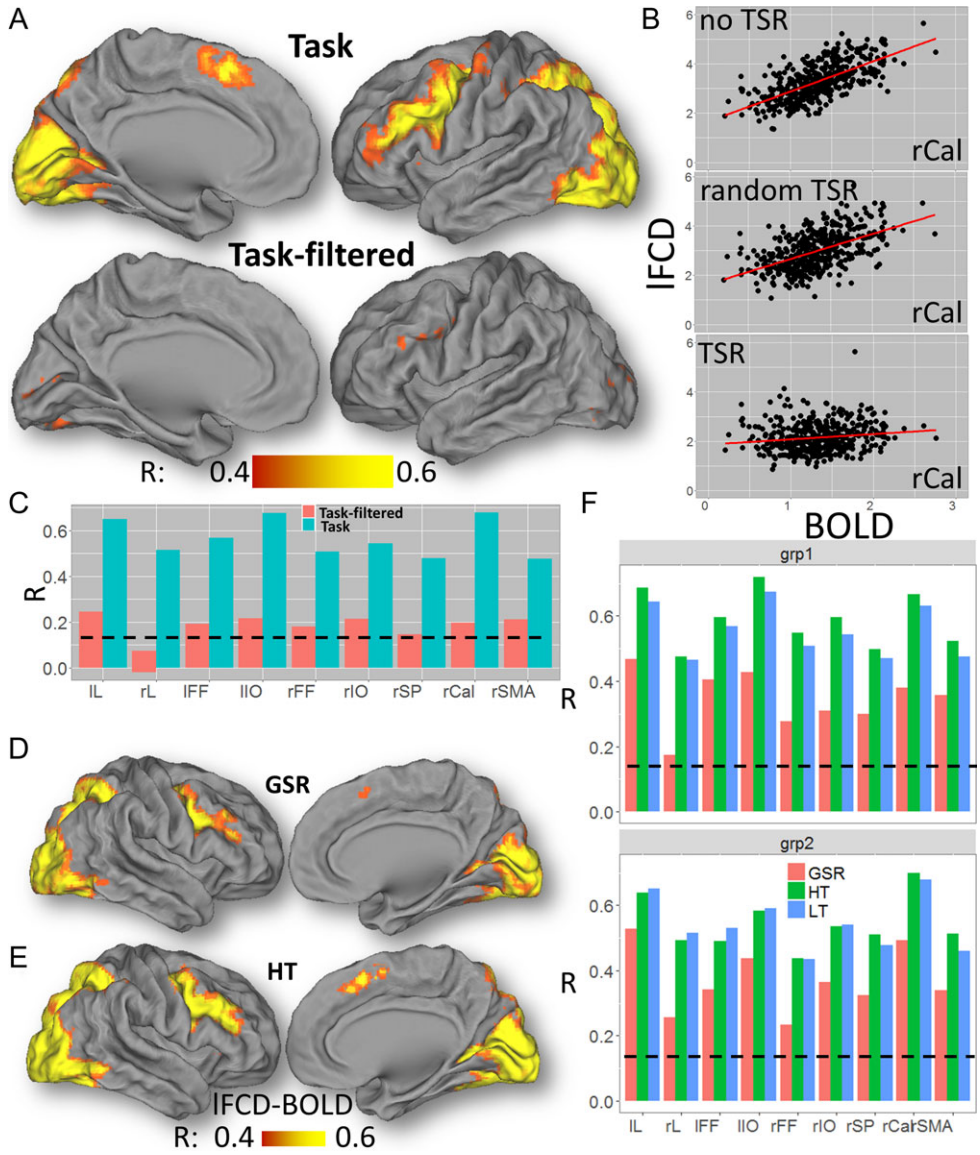

Figure 5. BOLD-lFCD correlation. (*A*) Voxelwise correlation across 426 subjects between lFCD and the BOLD signal during the Relational task, superimposed on medial and lateral views of the left cortical hemisphere of the PALS-B12 atlas of the cerebral cortex. (*B*) Scatter plots showing a stronger linear association between lFCD and BOLD signals (% change) in the right pericalcarine cortex (*r*Cal) for task (without TSR, R = 0.64; random TSR, R = 0.56) than for "task-filtered" (with TSR; R = 0.20) conditions. (*C*) Similar results were obtained for all ROIs. Voxelwise correlation maps across 426 subjects between the BOLD signal and lFCD computed with global signal regression (*D*) and with the high correlation threshold (*E*) for the Relational Task. (*F*) Bar plot showing that for all ROIs the correlation between lFCD and BOLD signals were similar for low (LT) and high (HT) correlation thresholds, and lower for lFCD computed with GSR compared to those without GSR. Black dashed line: $P < 0.05$, corrected for 9 ROIs (Bonferroni), 2-tailed. *l*L and *r*L: left and right lingual gyri; *l*IO and *r*IO: left and right inferior occipital gyri; *l*FF and *r*FF: left and right fusiform gyri; *r*SP: right superior parietal cortex; and *r*SMA: right supplementary motor area. Similar results were obtained for the Social task (not shown).

lFCD Versus ALFF

For the Relational (Fig. 7) and Social (not shown) tasks and for all ROIs, ΔALFF was linearly associated with ΔlFCD, and ALFF was associated with lFCD in the task-filtered condition.

BOLD Activation, Connectivity, and Behavior

Head motion (FD) showed significant correlation with the % BOLD signal change elicited by the tasks and all connectivity metrics in the pericalcarine cortex, effects that were strongest for ALFF (Figs S13 and S14). During the Relational task, FD showed strong correlation with ALFF ($R = 0.59$) and weak correlation with BOLD ($R = -0.18$) in the pericalcarine cortex ($P < 1E\text{-}04$); the negative association between FD and lFCD ($R = -0.12$) did not reach significance after corrections for multiple comparisons ($P = 0.013$). During the Social task, FD showed strong correlation with ALFF ($R = 0.46$) and weak correlation with lFCD ($R = -0.16$) in the pericalcarine cortex. Accuracy during the Relational task showed significant correlation with the %BOLD signal change elicited by the task and with all connectivity metrics in the pericalcarine cortex ($0.14 < abs(R) < 0.30$, $P < 0.05$, Bonferroni corrected for 12 comparisons, that is, 4 functional metrics × 3 behavioral metrics). With TSR, there was no significant correlation between accuracy during the Relational task and lFCD ($R = -0.04$); however, those for ALFF remained

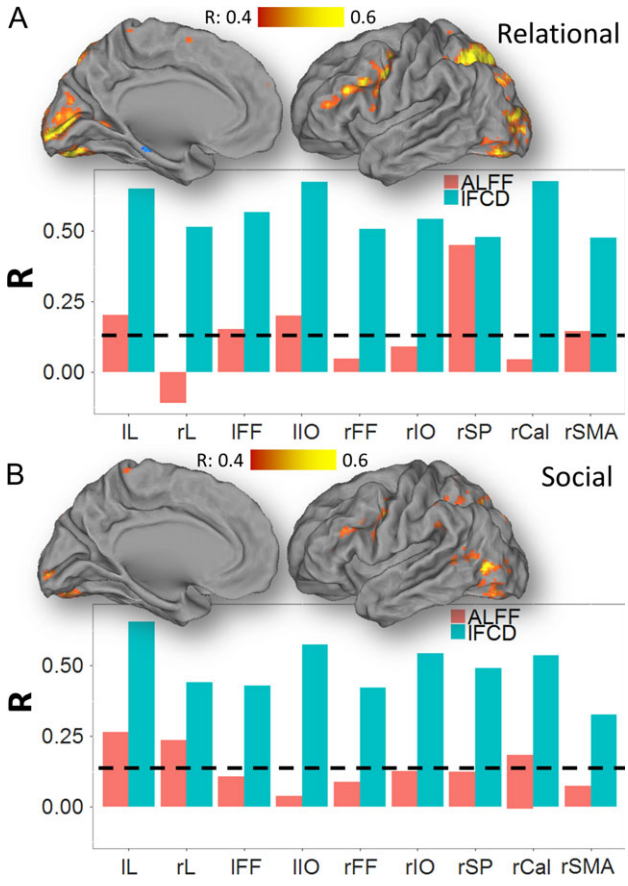

Figure 6. BOLD–ALFF correlation. Correlations between task-related changes in the BOLD signal with changes in ALFF, superimposed on medial and lateral views of the left cortical hemisphere of the PALS-B12 atlas of the cerebral cortex for the Relational (*A*) and Social (*B*) tasks. Bar plots show weaker correlations with BOLD signals for ALFF than for lFCD across tasks and ROIs. Black dashed line: $P < 0.05$, corrected for 9 ROIs (Bonferroni), 2-tailed. *l*L and *r*L: left and right lingual gyri; *l*IO and *r*IO: left and right inferior occipital gyri; lFF and *r*FF: left and right fusiform gyri; *r*SP: right superior parietal cortex; and *r*SMA: right supplementary motor area. Sample: 426 subjects.

significant with TSR ($|R| > 0.16$; Fig. S15). During the Social task, accuracy did not show significant correlation with any of the functional metrics, which might have reflected a performance ceiling effect for this task. Reaction time did not show correlation with any of the functional metrics for neither of the tasks.

Relational and Social Contrasts

In order to assess the effects of an individual epoch on lFCD we regressed out the effect of the other epoch on the time series using the TSR approach and computed lFCD from residual time series. During the Relational task, "relation" epochs caused increased lFCD bilaterally in occipital, inferior parietal, frontal and orbitofrontal and inferior temporal cortices, insula end cerebellum, compared to "match" epochs (Figs 8, S16; Table S1; $P_{FWE} < 1E\text{-}04$). Similar regions demonstrated increased BOLD–fMRI activation for "relation" epochs compared to "match" epochs (Table S2). In the somatosensory cortex, superior temporal gyrus, and occipitoparietal junction, however, "match" epochs caused stronger activation than "relation" epochs, which was not highlighted by lFCD. During the Social task, "social" epochs caused increased lFCD bilaterally in cuneus, inferior and middle occipital and temporal, and inferior frontal cortices, and increased BOLD–fMRI activation in cerebellum, amygdala, fusiform, inferior occipital and frontal, and inferior and middle temporal gyri, compared to the "random" condition (Fig. S17; Tables S3 and S4; $P_{FWE} < 1E\text{-}04$). In the premotor cortex, cingulum, dorsolateral prefrontal, posterior parietal, and medial occipital regions, "random" epochs caused stronger BOLD signals than "social" epochs (Figs S15) which was not highlighted by lFCD. These differential effects between epochs of the Relational and Social tasks were highly reproducible across groups (Figs S16 and S17).

Discussion

The neurovascular origin for the FC metrics derived from fMRI is still controversial (Birn et al. 2006; Shmueli et al. 2007; Shmuel and Leopold 2008; Logothetis et al. 2009; Magri et al. 2012; Di et al. 2013; Schölvinck et al. 2010; Power et al. 2012; Van Dijk et al. 2012). By systematically comparing the BOLD activation responses to tasks with the corresponding changes in connectivity metrics, and assuming the neurovascular origin of the BOLD signal (Logothetis et al. 2001), we provide indirect evidence for the neurovascular origin for ALFF and lFCD. Specifically, a robust correlation between BOLD signal elicited by the tasks and lFCD emerged from 2 different fMRI tasks and a large group of subjects from the HCP 500 Subjects data release. This is consistent with preclinical studies documenting correlations between spontaneous BOLD activity and neuronal activity as measured with local field potentials (Shmuel and Leopold 2008; Schölvinck et al. 2010; Magri et al. 2012). It is also consistent with human studies showing a correlation between measures of FC and cerebral blood flow (Liang et al. 2013) and regional brain glucose metabolism (Tomasi et al. 2013), which serve as markers of brain function (Sokoloff et al. 1977; Ugurbil 2016). Along with prior studies, our findings provide evidence that "resting-state" connectivity metrics such as lFCD reflect neurovascular activity presumably originated by fluctuations in neuronal activity (Du et al. 2014).

Despite evidence that connectivity metrics such as lFCD or ALFF are sensitive to brain states (Tomasi et al. 2014) and disease pathology (Tomasi and Volkow 2012a, 2014), they could also be influenced by regional differences in vascularization (Logothetis et al. 2009) and therefore reflect correlations driven by regional vascular structures devoid of functional meaning. The strong correlation between the BOLD signals elicited by the tasks and the lFCD is the main finding of the present study. Our results are consistent with the local connectivity increases observed in activated regions during a continuous semantic classification task compared to a resting-state condition (Sepulcre et al. 2010). The present study quantifies the coupling between the BOLD response and lFCD and ALFF during 2 different tasks (Relational and Social) using a novel TSR approach that allowed us to study effects of task epochs on local brain synchrony. The significant attenuation of the correlation between lFCD and BOLD after the removal of task-related signal modulations (i.e., TSR) indicates that lFCD reflects bulk (task-related) BOLD changes, likely of neurovascular origin. Mechanistically, fMRI task performance enhanced the synchrony of the local fMRI signals, increasing lFCD and ALFF in activated regions. Whereas the blocked nature of the tasks may have facilitated the analysis of task-related modulations, the proposed TSR approach should be applicable to event-related fMRI paradigms. Note similar approaches have been used to study FC in task conditions (Fair et al. 2007; Di et al. 2015). Since both tasks paradigms had significant power within the band of interest of

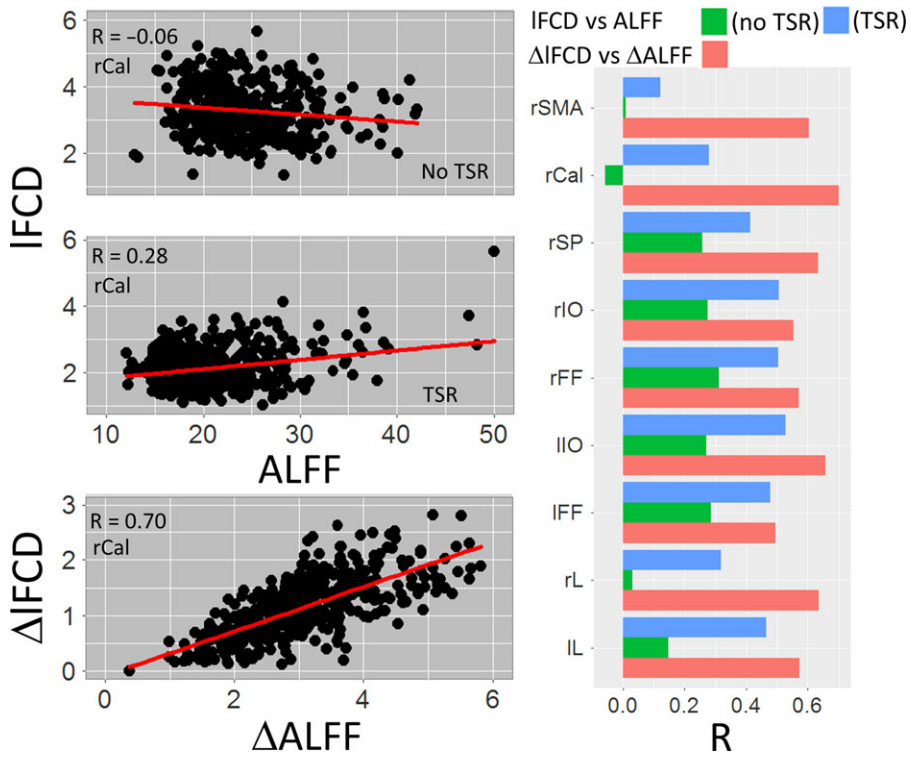

Figure 7. lFCD–ALFF correlation. Point plots (left) showing the linear association between lFCD and ALFF for task (no TSR) and task-filtered (TSR) conditions, as well as between task-related changes in lFCD and ALFF. Bar plots (right) show stronger correlations for task-related changes (red) than for task (green) and task-filtered (blue) conditions in all ROIs. Relational task; lL and rL: left and right lingual gyri; lIO and rIO: left and right inferior occipital gyri; lFF and rFF: left and right fusiform gyri; rSP: right superior parietal cortex; and rSMA: right supplementary motor area. Sample: 426 subjects.

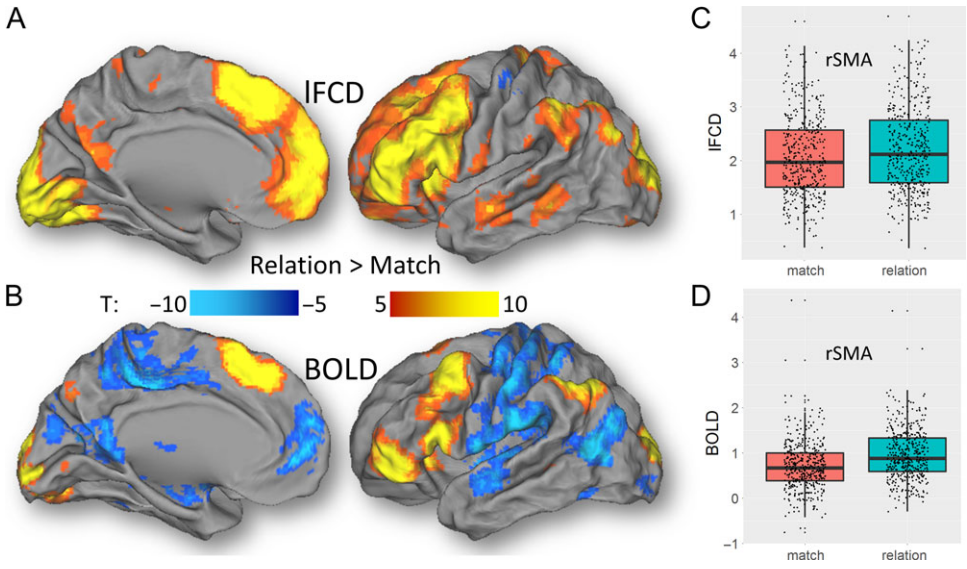

Figure 8. Differential effects of "relation" and "match" epochs on lFCD and BOLD. Statistical significance of differential lFCD (*A*) and differential BOLD signals (*B*) between the "relation" and "match" epochs of the Relational task across subjects, superimposed on medial and lateral views of the left cortical hemisphere of the PALS-B12 atlas of the cerebral cortex. The boxplots on the left highlight the average lFCD (*C*) and BOLD signals (*D*) within an exemplary anatomical ROI (rSMA: right supplementary motor area) for "relation" and "match" epochs of the Relational task across 426 subjects. SPM12 paired *t*-test.

low-frequency fluctuations, we expected that reducing the in-band power of intrinsically correlated signals would change the results in activated regions. Indeed, the task-filtering approach reduced lFCD and its correlation with BOLD signals in activated areas.

Brain activation to the Relational task showed significant correlation across subjects with the lFCD computed after TSR. This is consistent with the linear association across ROIs between lFCD metrics computed with or without TSR, and with the correlation across subjects between task-related lFCD

changes and BOLD responses. This indicates that in the absence of modulations induced by task performance, lFCD predicts BOLD activation patterns as was recently shown for other FC metrics (Tavor et al. 2016; Chan et al. 2017). This is consistent with the notion that regions with high FC are more likely to activate during cognitive tasks (Bertolero et al. 2015).

Here we show linear associations between ALFF and lFCD during task-filtered conditions (with TSR), and between ΔALFF and ΔlFCD, which are consistent with the correlations between ALFF and lFCD that we previously documented for the resting-state (Tomasi et al. 2016b). The weaker association between the metrics without TSR suggests that ALFF and lFCD map different functional properties. Specifically, since ALFF has strong vascular characteristics (Di et al. 2013) it is possible that in absence of filtering (TSR) the task-related modulations in MRI signals arising from large draining/pial veins have stronger effect for ALFF than for lFCD. Fractional ALFF (fALFF) was proposed as a less sensitive metric to physiologic noise (Zou et al. 2008). The degree to which our findings for ALFF are applicable to fALFF is uncertain. However, previous fMRI studies with the stop signal task did not show associations between brain activation and task-filtered fALFF (Zhang and Li 2010).

We also show that GSR significantly reduced the association between BOLD and lFCD, compared to no-GSR. Thus, attempts to reduce noise by GSR might have caused attenuation of meaningful neurophysiological signals. The relative proportion of neurophysiological signals and noise in the whole-brain fMRI signal is unknown (Liu 2013). At rest as well as during controlled manipulation of the end-tidal partial pressure of carbon dioxide (PCO2), the whole-brain signal is associated with the temporal variability in PCO2 (Corfield et al. 2001; Wise et al. 2004). Thus regression of the whole-brain signal could provide a relatively simple approach to minimize the effects of PCO2 variation, which is a predominant source of physiological noise in the BOLD signal (Wise et al. 2004; Chang and Glover 2009). However, the use of GSR has been controversial during the last 20 years because the contribution to the whole-brain signal from the activation of multiple coherent networks is unknown (Aguirre et al. 1998). Our results are consistent with previous fMRI studies, which noted that regression of the whole-brain signal can lead to different results, reduce sensitivity, and cause spurious deactivations for tasks that activate large whole brain networks (Aguirre et al. 1997, 1998; Desjardins et al. 2001). Previous studies evaluated the impact of GSR on local connectivity (Saad et al. 2012), and the neurophysiological origin of the resting-state global signal (Schölvinck et al. 2010). A recent study in nonhuman primates showed that reversible inactivation of the nucleus basalis of Maynert reduced the resting-state global signal but it did not affect the architecture of resting-state functional networks (Turchi et al. 2018). The reductions in task-based connectivity after GSR in the present study reflect attenuation of large task-induced BOLD signals and do not address potential effects of GSR on resting-state FC.

Accuracy showed significant correlation with %BOLD signal change elicited by the Relational task and with the changes in the connectivity metrics obtained during the task, which is consistent with prior findings showing associations between resting FC and accuracy (King et al. 2015; Chong et al. 2017). After BOLD signal modulation removal (i.e., TSR), the correlations between accuracy and lFCD vanished, whereas those for ALFF remained significant. Since both BOLD and lFCD showed correlation with accuracy during task but not after TSR, the task-related BOLD signal modulations could be the predominant mechanism supporting the associations between accuracy and lFCD. Since the correlations with accuracy for ALFF were not significantly affected by TSR, its association with accuracy could reflect other mechanisms. Specifically, ALFF might reflect a fundamental property of the neuronal organization that modulates function (and hence task performance), which is consistent with prior studies showing an association between resting FC and BOLD activation responses to various types of tasks (Di et al. 2013; Chan et al. 2017). However, the fact that there were no associations between connectivity metrics and accuracy for the Social task suggests that their sensitivity to accuracy is tasks-specific. For the Social task, this association could also occur in subcortical regions for which the HCP functional images have low sensitivity (Anteraper et al. 2013).

This is the first study to show differential effects of TSR across connectivity metrics. Specifically, TSR decreased ALFF in the whole brain and attenuated lFCD in activated brain regions. We observed these effects robustly at multiple levels (i.e., individual subject, groups of subjects, different tasks). They were normally distributed across subjects in all brain regions, supporting the use of parametric statistics.

Despite the effort to remove subjects with excessive head motion (i.e., subjects with FD > 0.4 mm), head motion showed significant correlation with the %BOLD signal change elicited by the tasks as well as all connectivity metrics, but predominantly with ALFF. These findings support the concerns in the neuroimaging community regarding the impact of head motion on FC metrics (Power et al. 2015) but show that after correction these effects are similar (except for ALFF) to those from BOLD–fMRI activation patterns.

Using TSR we also assessed the effects of individual epochs on lFCD, an approach that is reminiscent of psychophysiological interactions (PPI) (Friston et al. 1997). For lFCD, the differential patterns between conditions (i.e., "relation" versus "match"; "social" vs. "random") mapped to a large extent into the corresponding regional brain activation patterns, which in turn were in overall agreement with those previously reported for the Relational and Social tasks used by the HCP (Barch et al. 2013). Specifically, the network activated by the "relation" > "match" contrast included the visual attention network (visual, parietal, and dorsolateral prefrontal cortices and the cerebellum), which are involved in cognitive performance, and BA 10, which is involved with relational processing (Green et al. 2006) and hence expected to show increased activation for "relation" than for "match" epochs (Smith et al. 2007). The "social" > "random" contrast engaged brain regions involved in biological motion (superior temporal), biological form (fusiform), mentalizing (prefrontal cortex), affective processing (insula and amygdala), and the mirror system (inferior–frontal cortex) involved in the understanding of others (Wheatley et al. 2007). The emergence of these networks from the combination of lFCD and TSR further supports the neurovascular origin of the lFCD and makes it possible to study the effects of task conditions on local functional synchrony of the brain at a macroscopic scale (the size of the MRI voxel). Observationally, one can also identify regions in which the differential lFCD and BOLD patterns did not agree with one another. Specifically, during the Relational task, lFCD did not show effects paralleling those of increased BOLD responses in somatosensory, temporal and occipital cortices for "match" compared to "relation" epochs. Similarly, during the Social task, lFCD did not show effects paralleling the increased BOLD responses in the right middle temporal gyrus for "social" compared to "random" epochs, and in premotor cortex, cingulum, dorsolateral prefrontal, posterior parietal and medial occipital regions for "random" compared to "social"

epochs. The origin of these differences is unclear but could reflect differential sensitivity to vascular effects between the lFCD and BOLD metrics.

The lFCD is a voxelwise (short-range) metric that can be computed a thousand times faster than similar (long-range) degree maps. To achieve ultrafast computation, lFCD computation is based on a growing algorithm that relies on a correlation threshold. Higher correlation threshold leads to faster computation and lFCD maps with lower dynamic range. Here we show that the association between task-related BOLD signal changes and lFCD did not differ significantly as a function of correlation thresholds ($R = 0.4$ or 0.6) in any ROI. This is consistent with prior studies showing the insensitivity of the lFCD results to variable thresholds (Tomasi et al. 2016a; Cohen et al. 2017), and suggests that our findings do not depend on the arbitrary selection of model parameters. The weaker correlation with the task-related BOLD signals for ALFF than for lFCD suggests a stronger influence of origins other than the neurovascular coupling for the task-related changes in ALFF (i.e., head motion). However, given the vascular nature of ALFF (Di et al. 2013), the task-related changes in ALFF could also reflect vascular effects from pial/draining veins.

Study Limitations

We studied the association between neuronal activity and FC only in a phenomenological way through correlations between BOLD response and connectivity metrics (i.e., "validation through BOLD") because studies on direct associations between neuronal activity and FC would have required invasive electrophysiology. The use of fMRI data for extracting functional brain networks is a practice that is increasingly expanding (Fornito et al. 2012; Sporns 2014). However, the utterly complex and unknown functional organization of the brain, and the sparsity of neural representations may limit the interpretation of the observed differences between tasks within the same region (Logothetis 2008).

In summary, our findings indicate a common source for BOLD responses, ALFF and lFCD in the human brain, which is consistent with the neurovascular origin of FC metrics. Our data also provides support for network models of task-evoked FC.

Supplementary Material

Supplementary material is available at *Cerebral Cortex* online.

Funding

This work was accomplished with support from the National Institute on Alcohol Abuse and Alcoholism (Y1AA-3009).

Notes

Conflict of interest: None declared.

References

Aguirre G, Zarahn E, D'Esposito M. 1997. Empirical analyses of BOLD fMRI statistics. II. Spatially smoothed data collected under null-hypothesis and experimental conditions. NeuroImage. 5:199–212.

Aguirre GK, Zarahn E, D'Esposito M. 1998. The inferential impact of global signal covariates in functional neuroimaging analyses. NeuroImage. 8:302–306.

Anteraper S, Whitfield-Gabrieli S, Keil B, Shannon S, Gabrieli J, Triantafyllou C. 2013. Exploring functional connectivity networks with multichannel brain array coils. Brain Connect. 3: 302–315.

Barch D, Burgess G, Harms M, Petersen S, Schlaggar B, Corbetta M, Glasser M, Curtiss S, Dixit S, Feldt C, et al. 2013. Function in the human connectome: task-fMRI and individual differences in behavior. NeuroImage. 80:169–189.

Bertolero M, Yeo B, D'Esposito M. 2015. The modular and integrative functional architecture of the human brain. Proc Natl Acad Sci USA. 112:E6798–E6807.

Birn R, Diamond J, Smith M, Bandettini P. 2006. Separating respiratory-variation-related fluctuations from neuronal-activity-related fluctuations in fMRI. NeuroImage. 31:1536–1548.

Biswal B, Hudetz A, Yetkin F, Haughton V, Hyde J. 1997. Hypercapnia reversibly suppresses low-frequency fluctuations in the human motor cortex during rest using echo-planar MRI. J Cereb Blood Flow Metab. 17:301–308.

Biswal B, Mennes M, Zuo X, Gohel S, Kelly C, Smith S, Beckmann C, Adelstein J, Buckner R, Colcombe S, et al. 2010. Toward discovery science of human brain function. Proc Natl Acad Sci USA. 107:4734–4739.

Biswal B, Yetkin F, Haughton V, Hyde J. 1995. Functional connectivity in the motor cortex of resting human brain using echo-planar MRI. Magn Reson Med. 34:537–541.

Caeyenberghs K, Siugzdaite R, Drijkoningen D, Marinazzo D, Swinnen S. 2015. Functional connectivity density and balance in young patients with traumatic axonal injury. Brain Connect. 5:423–432.

Castelli F, Happé F, Frith U, Frith C. 2000. Movement and mind: a functional imaging study of perception and interpretation of complex intentional movement patterns. NeuroImage. 12:314–325.

Chan M, Alhazmi F, Park D, Savalia N, Wig G. 2017. Resting-state network topology differentiates task signals across the adult life span. J Neurosci. 37:2734–2745.

Chang C, Glover G. 2009. Relationship between respiration, end-tidal CO2, and BOLD signals in resting-state fMRI. NeuroImage. 47:1381–1393.

Chang C, Liu Z, Chen M, Liu X, Duyn J. 2013. EEG correlates of time-varying BOLD functional connectivity. NeuroImage. 72: 227–236.

Chong J, Ng G, Lee S, Zhou J. 2017. Salience network connectivity in the insula is associated with individual differences in interoceptive accuracy. Brain Struct Funct. 222: 1635–1644.

Cohen A, Tomasi D, Shokri-Kojori E, Nencka A, Wang Y. 2017. Functional connectivity density mapping: comparing multiband and conventional EPI protocols. Brain Imaging Behav. doi:10.1007/s11682-11017-19742-11687[Epub ahead of print].

Cordes D, Haughton V, Arfanakis K, Carew J, Turski P, Moritz C, Quigley M, Meyerand M. 2001. Frequencies contributing to functional connectivity in the cerebral cortex in "resting-state" data. AJNR Am J Neuroradiol. 22:1326–1333.

Corfield D, Murphy K, Josephs O, Adams L, Turner R. 2001. Does hypercapnia-induced cerebral vasodilation modulate the hemodynamic response to neural activation? NeuroImage. 13:1207–1211.

Desjardins A, Kiehl K, Liddle P. 2001. Removal of confounding effects of global signal in functional MRI analyses. NeuroImage. 13:751–758.

Di X, Fu Z, Chan S, Hung Y, Biswal B, Zhang Z. 2015. Task-related functional connectivity dynamics in a block-designed visual experiment. Front Hum Neurosci. 9:543.

Di X, Kannurpatti S, Rypma B, Biswal B. 2013. Calibrating BOLD fMRI activations with neurovascular and anatomical constraints. Cereb Cortex. 23:255–263.

Ding J, An D, Liao W, Wu G, Xu Q, Zhou D, Chen H. 2014. Abnormal functional connectivity density in psychogenic non-epileptic seizures. Epilepsy Res. 108:1184–1194.

Du C, Volkow N, Koretsky A, Pan Y. 2014. Low-frequency calcium oscillations accompany deoxyhemoglobin oscillations in rat somatosensory cortex. Proc Natl Acad Sci USA. 111: E4677–E4686.

Eklund A, Nichols T, Knutsson H. 2016. Cluster failure: why fMRI inferences for spatial extent have inflated false-positive rates. Proc Natl Acad Sci USA. 113:7900–7905.

Fair D, Schlaggar B, Cohen A, Miezin F, Dosenbach N, Wenger K, Fox M, Snyder A, Raichle M, Petersen S. 2007. A method for using blocked and event-related fMRI data to study "resting state" functional connectivity. NeuroImage. 35:396–405.

Fornito A, Harrison B, Zalesky A, Simons J. 2012. Competitive and cooperative dynamics of large-scale brain functional networks supporting recollection. Proc Natl Acad Sci USA. 109:12788–12793.

Fox M, Snyder A, Zacks J, Raichle M. 2006. Coherent spontaneous activity accounts for trial-to-trial variability in human evoked brain responses. Nat Neurosci. 9:23–25.

Friston K, Buechel C, Fink G, Morris J, Rolls E, Dolan R. 1997. Psychophysiological and modulatory interactions in neuroimaging. NeuroImage. 6:218–229.

Glasser M, Sotiropoulos S, Wilson J, Coalson T, Fischl B, Andersson J, Xu J, Jbabdi S, Webster M, Polimeni J, et al. 2013. The minimal preprocessing pipelines for the Human Connectome Project. NeuroImage. 80:105–124.

Gordon E, Laumann T, Adeyemo B, Huckins J, Kelley W, Petersen S. 2016. Generation and evaluation of a cortical area parcellation from resting-state correlations. Cereb Cortex. 26:288–303.

Green A, Fugelsang J, Kraemer D, Shamosh N, Dunbar K. 2006. Frontopolar cortex mediates abstract integration in analogy. Brain Res. 1096:125–137.

Greicius M. 2008. Resting-state functional connectivity in neuropsychiatric disorders. Curr Opin Neurol. 21:424–430.

King D, de Chastelaine M, Elward R, Wang T, Rugg M. 2015. Recollection-related increases in functional connectivity predict individual differences in memory accuracy. J Neurosci. 35:1763–1772.

Klingner C, Hasler C, Brodoehl S, Witte O. 2010. Dependence of the negative BOLD response on somatosensory stimulus intensity. NeuroImage. 53:189–195.

Konova A, Moeller S, Tomasi D, Goldstein R. 2015. Effects of chronic and acute stimulants on brain functional connectivity hubs. Brain Res. doi:10.1016/j.brainres.2015.1002.1002.

Lang X, Liu H, Qin W, Zhang Y, Xuan Y, Yu C. 2015. Brain functional connectivity density and individual fluid reasoning capacity in healthy young adults. NeuroReport. 26: 17–21.

Li S, Biswal B, Li Z, Risinger R, Rainey C, Cho J, Salmeron B, Stein E. 2000. Cocaine administration decreases functional connectivity in human primary visual and motor cortex as detected by functional MRI. Magn Reson Med. 43:45–51.

Liang X, Zou Q, He Y, Yang Y. 2013. Coupling of functional connectivity and regional cerebral blood flow reveals a physiological basis for network hubs of the human brain. Proc Natl Acad Sci USA. 110:1929–1934.

Liu T. 2013. Neurovascular factors in resting-state functional MRI. NeuroImage. 80:339–348.

Liu B, Fan L, Cui Y, Zhang X, Hou B, Li Y, Qin W, Wang D, Yu C, Jiang T. 2015. DISC1 Ser704Cys impacts thalamic-prefrontal connectivity. Brain Struct Funct. 220:91–100.

Logothetis N. 2008. What we can do and what we cannot do with fMRI. Nature (London). 453:869–878.

Logothetis N, Murayama Y, Augath M, Steffen T, Werner J, Oeltermann A. 2009. How not to study spontaneous activity. NeuroImage. 45:1080–1089.

Logothetis N, Pauls J, Augath M, Trinath T, Oeltermann A. 2001. Neurophysiological investigation of the basis of the fMRI signal. Nature. 412:150–157.

Magri C, Schridde U, Murayama Y, Panzeri S, Logothetis N. 2012. The amplitude and timing of the BOLD signal reflects the relationship between local field potential power at different frequencies. J Neurosci. 32:1395–1407.

Murnane K, Gopinath K, Maltbie E, Daunais J, Telesford Q, Howell L. 2015. Functional connectivity in frontal-striatal brain networks and cocaine self-administration in female rhesus monkeys. Psychopharmacology (Berl). 232:745–754.

Power J, Barnes K, Snyder A, Schlaggar B, Petersen S. 2012. Spurious but systematic correlations in functional connectivity MRI networks arise from subject motion. NeuroImage. 59:2142–2154.

Power J, Schlaggar B, Petersen S. 2015. Recent progress and outstanding issues in motion correction in resting state fMRI. NeuroImage. 105:536–551.

Qin W, Xuan Y, Liu Y, Jiang T, Yu C. 2015. Functional connectivity density in congenitally and late blind subjects. Cereb Cortex. 25:2507–2516.

Rack-Gomer A, Liau J, Liu T. 2009. Caffeine reduces resting-state BOLD functional connectivity in the motor cortex. NeuroImage. 46:56–63.

Saad Z, Gotts S, Murphy K, Chen G, Jo H, Martin A, Cox R. 2012. Trouble at rest: how correlation patterns and group differences become distorted after global signal regression. Brain Connect. 2:25–32.

Schölvinck M, Maier A, Ye F, Duyn J, Leopold D. 2010. Neural basis of global resting-state fMRI activity. Proc Natl Acad Sci USA. 107:10238–10243.

Sepulcre J, Liu H, Talukdar T, Martincorena I, Yeo B, Buckner R. 2010. The organization of local and distant functional connectivity in the human brain. PLoS Comput Biol. 6:e1000808.

Shmuel A, Leopold D. 2008. Neuronal correlates of spontaneous fluctuations in fMRI signals in monkey visual cortex: implications for functional connectivity at rest. Hum Brain Mapp. 29:751–761.

Shmueli K, van Gelderen P, de Zwart J, Horovitz S, Fukunaga M, Jansma J, Duyn J. 2007. Low-frequency fluctuations in the cardiac rate as a source of variance in the resting-state fMRI BOLD signal. NeuroImage. 38:306–320.

Singh K, Fawcett I. 2008. Transient and linearly graded deactivation of the human default-mode network by a visual detection task. NeuroImage. 41:100–112.

Smith S, Beckmann C, Andersson J, Auerbach E, Bijsterbosch J, Douaud G, Duff E, Feinberg D, Griffanti L, Harms M, et al. 2013. Resting-state fMRI in the Human Connectome Project. NeuroImage. 80:144–168.

Smith R, Keramatian K, Christoff K. 2007. Localizing the rostrolateral prefrontal cortex at the individual level. NeuroImage. 36:1387–1396.

Sokoloff L, Reivich M, Kennedy C, Des Rosiers M, Patlak C, Pettigrew K, Sakurada O, Shinohara M. 1977. The [14C]deoxyglucose method for the measurement of local cerebral glucose utilization: theory, procedure, and normal values in the

conscious and anesthetized albino rat. J Neurochem. 28: 897–916.
Sporns O. 2014. Contributions and challenges for network models in cognitive neuroscience. Nat Neurosci. 17:652–660.
Tavor I, Parker Jones O, Mars R, Smith S, Behrens T, Jbabdi S. 2016. Task-free MRI predicts individual differences in brain activity during task performance. Science. 352:20216–20352.
Tian T, Qin W, Liu B, Jiang T, Yu C. 2013. Functional connectivity in healthy subjects is nonlinearly modulated by the COMT and DRD2 polymorphisms in a functional system-dependent manner. J Neurosci. 33:17519–17526.
Tomasi D, Ernst T, Caparelli E, Chang L. 2006. Common deactivation patterns during working memory and visual attention tasks: an intra-subject fMRI study at 4 Tesla. Hum Brain Mapp. 27:694–705.
Tomasi D, Shokri-Kojori E, Volkow N. 2016a. High-resolution functional connectivity density: hub locations, sensitivity, specificity, reproducibility, and reliability. Cereb Cortex. 26:3249–3259.
Tomasi D, Shokri-Kojori E, Volkow N. 2016b. Temporal changes in local functional connectivity density reflect the temporal variability of the amplitude of low frequency fluctuations in gray matter. PLoS One. 11:e0154407.
Tomasi D, Volkow N. 2010. Functional connectivity density mapping. Proc Natl Acad Sci USA. 107:9885–9890.
Tomasi D, Volkow N. 2011. Gender differences in brain functional connectivity density. Hum Brain Mapp. 33:849–860.
Tomasi D, Volkow N. 2012a. Abnormal functional connectivity in children with attention-deficit/hyperactivity disorder. Biol Psychiatry. 71:443–450.
Tomasi D, Volkow N. 2012b. Aging and functional brain networks. Mol Psychiatry. 17:549–558.
Tomasi D, Volkow N. 2014. Mapping small-world properties through development in the human brain: disruption in schizophrenia. PLoS One. 9:e96176.
Tomasi D, Wang G, Volkow N. 2013. Energetic cost of brain functional connectivity. Proc Natl Acad Sci USA. 110:13642–13647.
Tomasi D, Wang R, Wang G, Volkow N. 2014. Functional connectivity and brain activation: a synergistic approach. Cereb Cortex. 24:2619–2629.
Turchi J, Chang C, Ye F, Russ B, Yu D, Cortes C, Monosov I, Duyn J, Leopold D. 2018. The basal forebrain regulates global resting-state fMRI fluctuations. Neuron. 97:940–952.
Tzourio-Mazoyer N, Landeau B, Papathanassiou D, Crivello F, Etard O, Delcroix N, Mazoyer B, Joliot M. 2002. Automated anatomical labeling of activations in SPM using a macroscopic anatomical parcellation of the MNI MRI single-subject brain. NeuroImage. 15:273–289.
Ugurbil K. 2016. What is feasible with imaging human brain function and connectivity using functional magnetic resonance imaging. Philos Trans R Soc Lond B Biol Sci. 371: 1705. 10.1098/rstb.2015.0361.
Uğurbil K, Xu J, Auerbach E, Moeller S, Vu A, Duarte-Carvajalino J, Lenglet C, Wu X, Schmitter S, Van de Moortele P, Strupp J, et al. 2013. Pushing spatial and temporal resolution for functional and diffusion MRI in the Human Connectome Project. NeuroImage. 80:80–104.
Van Dijk K, Sabuncu M, Buckner R. 2012. The influence of head motion on intrinsic functional connectivity MRI. NeuroImage. 59:431–438.
Van Essen D. 2005. A population-average, landmark- and surface-based (PALS) atlas of human cerebral cortex. NeuroImage. 28:635–662.
Vélez-Hernández M, Padilla E, Gonzalez-Lima F, Jiménez-Rivera C. 2014. Cocaine reduces cytochrome oxidase activity in the prefrontal cortex and modifies its functional connectivity with brainstem nuclei. Brain Res. 1542:56–69.
Walter S, Forsgren M, Lundengård K, Simon R, Torkildsen Nilsson M, Söderfeldt B, Lundberg P, Engström M. 2016. Positive allosteric modulator of GABA lowers BOLD responses in the cingulate cortex. PLoS One. 11:e0148737.
Wheatley T, Milleville S, Martin A. 2007. Understanding animate agents: distinct roles for the social network and mirror system. Psychol Sci. 18:469–474.
Whitfield-Gabrieli S, Nieto-Castanon A. 2012. Conn: a functional connectivity toolbox for correlated and anticorrelated brain networks. Brain Connect. 2:125–141.
Wise R, Ide K, Poulin M, Tracey I. 2004. Resting fluctuations in arterial carbon dioxide induce significant low frequency variations in BOLD signal. NeuroImage. 21:1652–1664.
Wong C, Olafsson V, Tal O, Liu T. 2012. Anti-correlated networks, global signal regression, and the effects of caffeine in resting-state functional MRI. NeuroImage. 63: 356–364.
Yang H, Long X, Yang Y, Yan H, Zhu C, Zhou X, Zang Y, Gong Q. 2007. Amplitude of low frequency fluctuation within visual areas revealed by resting-state functional MRI. NeuroImage. 36:144–152.
Zhang S, Li C. 2010. A neural measure of behavioral engagement: task-residual low-frequency blood oxygenation level-dependent activity in the precuneus. NeuroImage. 49:1911–1918.
Zhuo C, Zhu J, Qin W, Qu H, Ma X, Tian H, Xu Q, Yu C. 2014. Functional connectivity density alterations in schizophrenia. Front Behav Neurosci. 8:404.
Zou Q, Zhu C, Yang Y, Zuo X, Long X, Cao Q, Wang Y, Zang Y. 2008. An improved approach to detection of amplitude of low-frequency fluctuation (ALFF) for resting-state fMRI: fractional ALFF. J Neurosci Methods. 172:137–141.